

Extended GeV-TeV Emission around Gamma-Ray Burst Remnants, and the Case of W49B

Kunihiro Ioka¹, Shiho Kobayashi^{1,2}, and Peter Mészáros^{1,2,3}

ABSTRACT

We investigate the high-energy photon emission around Gamma-Ray Burst (GRB) remnants caused by ultrahigh-energy cosmic rays (UHECRs) from the GRBs. We apply the results to the recent report that the supernova remnant W49B is a GRB remnant in our Galaxy. If this is correct, and if GRBs are sources of UHECRs, a natural consequence of this identification would be a detectable TeV photon emission around the GRB remnant. The imaging of the surrounding emission could provide new constraints on the jet structure of the GRB.

Subject headings: cosmic rays — gamma rays: bursts — gamma rays: theory

1. Introduction

Past Gamma-Ray Burst (GRB) occurrences in our galaxy may have left radio remnants resembling hyperenergetic supernovae (e.g., Perna & Loeb 2000). Recently, Chandra X-ray observations have led to infer that the supernova remnant W49B (G43.3-0.2) may be the first remnant of a GRB discovered in the Milky Way.⁴ This remnant is located at $d \sim 10$ kpc from earth, has a radius of $R \sim 10$ pc, and is estimated to have occurred ~ 3000 yr ago in our Galaxy.

In this Letter we discuss the high energy implications of the GRB origin of some supernova-like remnants, and in particular of the assumption that W49B is a GRB remnant. We show that, if we also assume that GRBs are sources of ultrahigh-energy cosmic

¹Physics Department and Center for Gravitational Wave Physics, 104 Davey Laboratory, Pennsylvania State University, University Park, PA 16802

²Department of Astronomy and Astrophysics, 525 Davey Laboratory, Pennsylvania State University, University Park, PA 16802

³The Institute for Advanced Study, Einstein Drive, Princeton, NJ 08540

⁴http://chandra.harvard.edu/press/04_releases/press_060204.html

rays (UHECRs), significant TeV gamma-ray emission may be detectable around W49B. A positive detection would verify not only that W49B is a GRB remnant, but also that the GRBs can efficiently accelerate UHECRs.

GRBs are one of the most promising candidates for the origin of UHECRs (Waxman 1995; Vietri 1995; Milgrom & Usov 1995). The physical conditions required in GRBs to produce MeV gamma-rays also allow protons to be accelerated up to $\sim 10^{20}$ eV. The energy generation rate per decade of UHECRs in the range 10^{19} - 10^{21} eV is similar to the γ -ray generation rate of GRBs in the BATSE energy band 0.02-2 MeV,

$$E_p^2 \frac{dn_p^{\text{CR}}}{dE_p} (10^{19} - 10^{21} \text{ eV}) \simeq \dot{\varepsilon}_{\gamma}^{\text{GRB}} (0.02 - 2 \text{ MeV}) , \quad (1)$$

and equation (1) is the common assumption made for GRBs as the sources of UHECRs (Waxman 2004; Vietri, De Marco, & Guetta 2003). Since photon emission is proportional to the square of the electron Lorentz factor, two decades in photon energy correspond to one decade in particle energy, but the electron (and proton) energy distribution would be expected to be broader than this. Also, additional photon energy is observed in many cases beyond the BATSE range. Thus equation (1) implying $\dot{\varepsilon}_{[10^{19}, 10^{21}] \text{ eV}}^{\text{CR}} \sim 3 \dot{\varepsilon}_{[0.02, 2] \text{ MeV}}^{\text{GRB}}$ reflects approximate equipartition between nucleon and electron energies; and larger nucleon energies relative to electrons would not be unreasonable (e.g., Wick, Dermer, & Atoyan 2004). Note that these energies refer to the prompt component, whereas snapshot fit and radio calorimetric energies refer to the afterglow. We note also that, for the purposes of this Letter, even UHECR of energies well below 10^{20} eV can lead to GeV-TeV photon emission.

If the GRBs are the origin of UHECRs, an unavoidable component of the UHECR outflow will be in the form of neutrons. This is due to conversion of protons into neutrons via photomeson interactions, $p\gamma \rightarrow n\pi^+$ on the GRB photons. The optical depth for this process is about a few for protons with energy $\gtrsim 10^{16}$ eV (Waxman & Bahcall 1997; Vietri 1998). Protons, unlike neutrons, feel the magnetic field in the ejecta and are subjected to adiabatic cooling as the ejecta expands (Rachen & Mészáros 1998), hence the neutron to proton ratio at similar energies could range from approximate equality to about 20% (Atoyan & Dermer 2001). These high energy neutrons decay into protons and electrons outside the ejecta, $n \rightarrow p + e^- + \bar{\nu}_e$, followed by interactions with the surroundings. This results in a photon, neutrino and neutron emission around the remnant (Dermer 2002; Biermann, Medina Tanco, Engel, & Pugliese 2004).

In this Letter we consider the photon emission from β -decay electrons, and discuss its detectability in particular for the W49B case. The TeV emission is probably detectable by the future atmospheric Cherenkov telescope VERITAS, while HEGRA may have already detected this signal in their archival data, if the GRB was intense, and we strongly urge the

reanalysis of the HEGRA database.

2. β -decay electron emission around the GRB remnant

We first consider each decade of neutron energy, to simplify the discussion. We assume that the GRB ejects neutrons with a Lorentz factor $\gamma_n \sim 10^8 \gamma_{n,8}$ and a total energy $E_n \sim 10^{50} E_{n,50}$ erg, at a time $t_{\text{age}} \sim 3000 t_{\text{age},3.5}$ yr ago (later we integrate over the energies). These neutrons decay, $n \rightarrow p + e^- + \bar{\nu}_e$, over

$$t_{\text{decay}} \sim \gamma_n t_\beta \sim 3 \times 10^3 \gamma_{n,8} \text{ yr}, \quad (2)$$

producing high energy electrons with a Lorentz factor $\gamma_e \sim \gamma_n$. Here $t_\beta \sim 900$ s is the β -decay time in the comoving frame. The energy of the β -decay electrons is $m_p/m_e \sim 10^3$ times smaller than that of the neutrons. We consider only electrons with $\gamma_e \sim \gamma_n \gtrsim 10^6$, from neutrons which decay outside the remnant, $ct_{\text{decay}} \gtrsim R$, so that we can easily separate the β -decay emission from the remnant emission, such as due to the pion decay (Enomoto et al. 2002).

The β -decay electrons radiate via synchrotron and the inverse Compton (IC) emission. The corresponding fluxes depend on the energy densities of the magnetic and photon fields. We adopt the typical magnetic field in our Galaxy $B \sim 3 \mu\text{G}$ corresponding to a magnetic energy density $U_B \sim 4 \times 10^{-13}$ erg cm $^{-3}$. For the IC process, we consider the cosmic microwave background (CMB) as the main target photons.⁵ The energy density and temperature of the CMB are about $U_{\text{CMB}} \sim 4 \times 10^{-13}$ erg cm $^{-3}$ and $\epsilon_{\text{CMB}} \sim 2.7$ K. The electron cooling time due to the combined emissions is

$$t_{\text{cool}}(\gamma_e) \sim \frac{3m_e c}{4\gamma_e \sigma_T U_{\text{total}}} \sim 1 \times 10^4 \gamma_{e,8}^{-1} U_{\text{total},-12}^{-1} \text{ yr}, \quad (3)$$

where $U_{\text{total}} = U_B + \bar{U}_{\text{CMB}} = 10^{-12} U_{\text{total},-12}$ erg cm $^{-3}$ is the total energy density, and we use $\bar{U}_{\text{CMB}} = U_{\text{CMB}} \min(1, m_e c^2 / 9\epsilon_{\text{CMB}} \gamma_e)$ to take the Klein-Nishina (KN) effect into account.⁶

There are two cases, depending on whether or not most of the neutrons decay within the remnant age, the latter case being divided into two sub-cases depending on whether or not the electrons cool slower than the remnant age, leading to three different types of emission region shape.

⁵Our calculations show that the IR and optical backgrounds with mean values are negligible.

⁶We numerically found that the IC spectrum νF_ν peaks at $\sim 9\epsilon_{\text{CMB}} \gamma_e^2$ in the Thomson regime.

(a) Fast decay, $t_{\text{decay}}(\gamma_e) < t_{\text{age}}$: In this case the fraction of neutrons that have decayed is $f_\beta \sim 1$. The radius of the emitting region is roughly equal to the β -decay length $\sim ct_{\text{decay}} \sim 0.9\gamma_{e,8}$ kpc, which is much larger than the Larmor radius of the β -decay electrons,

$$r_L \sim \frac{\gamma_e m_e c^2}{qB} \sim 6 \times 10^{-2} \gamma_{e,8} B_{-6}^{-1} \text{ pc}, \quad (4)$$

where $B = 10^{-6} B_{-6}$ G. Thus, the sky distribution of the emitting region is roughly preserved, as shown in Figure 1 (a). The emitting region has an elongated shape on the sky, whose solid angle is approximately

$$\Omega \sim 4\theta(ct_{\text{decay}}/d)^2 \sim (1\theta_{-1}\gamma_{e,8})^\circ \times (10\gamma_{e,8})^\circ \sim 3 \times 10^{-3} \theta_{-1} \gamma_{e,8}^2 \text{ sr}, \quad (5)$$

if the opening half-angle of the jet is $\theta = 0.1\theta_{-1}$. Note that the neutrons are beamed into a jet because of the relativistic beaming.

An electron with an initial cooling time $t_{\text{cool}}(\gamma_e) < t_{\text{age}}$ cools down to the Lorentz factor determined by $t_{\text{cool}}(\gamma_e) \sim t_{\text{age}}$. Thus the current Lorentz factor of electrons is given by

$$\hat{\gamma}_e \sim \min\left(\gamma_e, \frac{3m_e c}{4t_{\text{age}} \sigma_T U_{\text{total}}}\right) \sim 1 \times 10^8 \min(\gamma_{e,8}, 3t_{\text{age},3.5}^{-1} U_{\text{total},-12}^{-1}). \quad (6)$$

Irrespective of the initial γ_e , the order of magnitude of the current Lorentz factor $\hat{\gamma}_e$ is the same in all the emitting region, so that the surface brightness on the sky depends weakly on the radius $\propto r^{-1}$, and it is nearly homogeneous.

The characteristic synchrotron frequency and the synchrotron peak flux at the observer are given by

$$\begin{aligned} \nu_m &= \frac{qB\hat{\gamma}_e^2}{2\pi m_e c} \sim 1 \times 10^2 B_{-6} \hat{\gamma}_{e,8}^2 \text{ eV}, \\ \nu F_\nu(\nu_m) &\sim \frac{m_e \hat{\gamma}_e}{m_p \gamma_e} \frac{U_B}{U_{\text{total}}} \frac{f_\beta E_n}{4\pi d^2 t_{\text{cool}}(\hat{\gamma}_e)} \sim 1 \times 10^{-11} f_\beta E_{n,50} U_{B,-12} \hat{\gamma}_{e,8}^2 \gamma_{e,8}^{-1} \text{ erg s}^{-1} \text{ cm}^{-2}. \end{aligned} \quad (7)$$

Similarly the characteristic IC frequency and the IC peak flux are

$$\begin{aligned} \nu_{\text{CMB}} &\sim \min(\hat{\gamma}_e m_e c^2, 9\epsilon_{\text{CMB}} \hat{\gamma}_e^2) \sim 50 \min(\hat{\gamma}_{e,8}, 2\epsilon_{\text{CMB},-3} \hat{\gamma}_{e,8}^2) \text{ TeV}, \\ \nu F_\nu(\nu_{\text{CMB}}) &\sim \frac{m_e \hat{\gamma}_e}{m_p \gamma_e} \frac{\bar{U}_{\text{CMB}}}{U_{\text{total}}} \frac{f_\beta E_n}{4\pi d^2 t_{\text{cool}}(\hat{\gamma}_e)} \sim 1 \times 10^{-11} f_\beta E_{n,50} \bar{U}_{\text{CMB},-12} \hat{\gamma}_{e,8}^2 \gamma_{e,8}^{-1} \text{ erg s}^{-1} \text{ cm}^{-2}, \end{aligned} \quad (8)$$

where $\epsilon_{\text{CMB}} = 10^{-3} \epsilon_{\text{CMB},-3}$ eV is the target photon energy. The surface brightness of emission is about $S = \nu F_\nu / \Omega \sim 5 \times 10^{-9} \theta_{-1}^{-1} E_{n,50} U_{-12} \hat{\gamma}_{e,8}^2 \gamma_{e,8}^{-3}$ erg s⁻¹ cm⁻² sr⁻¹.

(b) Slow decay, $t_{\text{decay}}(\gamma_e) > t_{\text{age}}$. In this case, almost all neutrons are still decaying. The radius of the emitting region is roughly $\sim ct_{\text{age}} \sim 1t_{\text{age},3.5}$ kpc, which is again larger than the

Larmor radius for our parameters. In this case, however, the shape of the emitting region depends on whether electrons cool within the remnant age or not.

(b1) If $t_{\text{cool}}(\gamma_e) > t_{\text{age}}$, the electrons do not cool much, so the current Lorentz factor of the electrons is $\hat{\gamma}_e \sim \gamma_e$. Thus the surface brightness of the emitting region is nearly homogeneous (see Figure 1 (b1)). The fraction of neutrons that have decayed is $f_\beta \sim t_{\text{age}}/t_{\text{decay}} \sim 1t_{\text{age},3.5}\gamma_{e,8}^{-1}$. The solid angle of the emitting region on the sky is about

$$\Omega \sim 4\theta(ct_{\text{age}}/d)^2 \sim (1\theta_{-1}t_{\text{age},3.5})^\circ \times (10t_{\text{age},3.5})^\circ \sim 4 \times 10^{-3}\theta_{-1}t_{\text{age},3.5}^2 \text{ sr.} \quad (9)$$

The synchrotron and IC emission is given by equations (7) and (8), respectively. The surface brightness of the emission is $S = \nu F_\nu/\Omega \sim 4 \times 10^{-9}\theta_{-1}^{-1}E_{n,50}U_{-12}t_{\text{age},3.5}^{-1} \text{ erg s}^{-1} \text{ cm}^{-2} \text{ sr}^{-1}$.

(b2) If $t_{\text{cool}}(\gamma_e) < t_{\text{age}}$, almost all the electrons cool down, except for a smaller fraction of electrons at the jet head which have not cooled yet because the neutrons are just decaying, $t_{\text{decay}}(\gamma_e) > t_{\text{age}}$. Although the number of these hot electrons is small, the flux from these hot electrons dominates that of the rest, since they have a larger energy and a shorter cooling time (see Figure 1 (b2)). Thus we concentrate on the hot electrons within the distance $\sim ct_{\text{cool}}(\gamma_e) \sim 3\gamma_{e,8}^{-1}U_{\text{total},-12}^{-1}$ kpc from the jet head. The current Lorentz factor of these electrons is $\hat{\gamma}_e \sim \gamma_e$, and the fraction of neutrons that have decayed is $f_\beta \sim t_{\text{cool}}/t_{\text{decay}} \sim 3\gamma_{e,8}^{-2}U_{\text{total},-12}^{-1}$. The solid angle of the emitting region on the sky is

$$\begin{aligned} \Omega &\sim 4\theta(ct_{\text{age}}/d)(ct_{\text{cool}}/d) \sim (1\theta_{-1}t_{\text{age},3.5})^\circ \times (30\gamma_{e,8}^{-1}U_{\text{total},-12}^{-1})^\circ \\ &\sim 1 \times 10^{-2}\theta_{-1}t_{\text{age},3.5}\gamma_{e,8}^{-1}U_{\text{total},-12}^{-1} \text{ sr.} \end{aligned} \quad (10)$$

The synchrotron and IC emission is given by equations (7) and (8), respectively. The surface brightness of the emission is about $S = \nu F_\nu/\Omega \sim 1 \times 10^{-9}\theta_{-1}^{-1}E_{n,50}U_{-12}t_{\text{age},3.5}^{-1} \text{ erg s}^{-1} \text{ cm}^{-2} \text{ sr}^{-1}$.

We may usually assume the emission to be isotropic in the lab-frame, since the Larmor radius is the minimum scale $r_L < \min(ct_{\text{cool}}, ct_{\text{age}})$ for almost all parameters. For $\gamma_e \gtrsim 10^{10} \min(2B_{-6}^{1/2}U_{\text{total},-12}^{-1/2}, 10^2B_{-6}t_{\text{age},3.5})$, however, the emission is beamed into the jet direction and the observed flux is reduced.

3. Detectability

We have numerically calculated the IC spectrum using equation (2.48) of Blumenthal & Gould (1970). We assume a blackbody CMB spectrum and a power-law neutron distribution $N(\gamma_n)d\gamma_n \propto \gamma_n^{-p}d\gamma_n$ with $p = 2$ for $10^7 \leq \gamma_n < 10^{11}$ and $p = 1$ for $\gamma_n < 10^7$ as expected in GRBs (Waxman & Bahcall 1997), and use $f_\beta N(\gamma_e < \hat{\gamma}_e)d\gamma_e$ as the distribution of emitting

electrons, where f_β includes the effects of the cooling and the partial neutron decay. We consider three cases for the normalization of $N(\gamma_e)$: (I) We set it equal to the geometrically corrected energy of equation (1), $\int_{10^{10}}^{10^{12}} \gamma_e m_n c^2 N(\gamma_e) d\gamma_e = 3 \times 10^{51}$ erg. (II) The same total energy is distributed over the entire range, $\int_1^{10^{11}} \gamma_e m_n c^2 N(\gamma_e) d\gamma_e = 3 \times 10^{51}$ erg. (III) The energy of case (II) is further reduced by a factor 5, considering that only $\sim 20\%$ of accelerated protons are converted to neutrons (Atoyan & Dermer 2001; Dermer & Atoyan 2004).

The emission from the β -decay electrons is extended, hence it competes with the diffuse background radiation. Since W49B resides in the Galactic disk $(l, b) = (43.3, -0.2)$, the disk emission is the main confusion source. We find that the IR-optical band (e.g., Bernstein, Freedman, & Madore 2002) and the X-ray band (Kaneda et al. 1997; Snowden et al. 1995) are not suitable for the detection of the β -decay emission considered here, because the diffuse background dominates. The MeV region (Kinzer, Purcell, & Kurfess 1999; Strong, Moskalenko, & Reimer 2000) could be a possible observing window, but appropriate detectors have not been developed in this band. Although INTEGRAL might be one possibility, the sub-MeV background may be difficult to subtract (Lebrun et al. 2004).

On the other hand, the GeV band (Hunter et al. 1997) and the TeV band appear to be suitable windows for the observation of β -decay IC emission. Strictly speaking, the diffuse background in the TeV band has not been detected. Only an upper limit exists (Aharonian et al. 2001; LeBohec et al. 2000; Amenomori et al. 2002). However the predicted background is below the power-law extrapolation of the upper limit (Aharonian & Atoyan 2000; Strong, Moskalenko, & Reimer 2004), so that it is probable that the TeV background is negligible.

We compare now the predicted GeV-TeV flux to the sensitivities of various detectors. Figure 2 shows the flux of the β -decay electrons and the sensitivities of GLAST, HEGRA, MAGIC⁷ and VERITAS (e.g., McEnery, Moskalenko, & Ormes 2004). Note that the northern sky location of W49B makes it an unsuitable target for some ground-based detectors, such as CANGAROO or HESS.

With HEGRA, MAGIC and VERITAS, whose angular resolution is $\sim 0.1^\circ$, the source size should be taken into account. Since the search region has to be expanded, more background is included. The sensitivity is proportional to the inverse square of the background, for background dominated counting statistics. Therefore the flux sensitivity of an atmospheric Cherenkov telescope to an extended source, F_ν^{extend} , is given by $F_\nu^{\text{extend}} = F_\nu^{\text{point}} (\Omega / \pi \theta_{\text{cut}}^2)^{1/2}$, where F_ν^{extend} is the sensitivity to a point source, and $\theta_{\text{cut}} \sim 0.1^\circ$ is the angular cut in the point source analysis (Konopelko, Lucarelli, Lampeitl, & Hofmann 2002;

⁷<http://hegra1.mppmu.mpg.de/MAGICWeb/>

Lessard, Buckley, Connaughton, & Le Bohec 2001). In Figure 2 the dashed lines show the corrected β -decay emission $\nu F_\nu (\Omega / \pi \theta_{\text{cut}}^2)^{-1/2}$, which should be compared with the detector sensitivity.

From Figure 2 we see that VERITAS might be likely to detect the β -decay emission. Even our most conservative case (III) is only a factor 2 below the VERITAS limit. MAGIC may also marginally detect the emission. GLAST appears unable to detect the signal, while the sensitivity of HEGRA is only a factor 2 above the flux of case (I). Thus, in the case of a stronger than average GRB (Wick, Dermer, & Atoyan 2004), the detection by HEGRA may not be implausible. In fact the observed total gamma-ray energy has a factor 2 dispersion (Bloom, Frail, & Kulkarni 2003).

HEGRA has actually observed the region including W49B (Aharonian et al. 2001, 2002). An upper limit on the TeV flux from W49B is given as ~ 0.14 Crab flux $\sim 7 \times 10^{-12}$ erg cm $^{-2}$ s $^{-1}$ (Aharonian et al. 2002). However this limit constrains the flux only in a $\sim 0.1^\circ$ circle centered on W49B, since the angular cut $\theta_{\text{cut}} \sim 0.1^\circ$ is applied in the analysis. Thus this limit is not stringent. In order to improve the sensitivity to the β -decay emission, we should expand the angular cut θ_{cut} so that all the β -decay emitting region is included in the analysis. The probable size is $\sim 0.1^\circ \times 1^\circ$, centered on W49B and with a shape as in Figure 1 (a), possibly along the direction in which more metals are ejected within W49B. Although HEGRA has ended observations, a reanalysis of the data on this region may constrain the β -decay emission.

4. Discussion

The possibility of imaging the β -decay emission region of a GRB remnant could open a novel way of constraining the structure of GRB jets. Currently jets are unresolved, but recent studies indicate that the jet structure is essential to an understanding the GRB phenomenon (Rossi, Lazzati, & Rees 2002; Zhang & Mészáros 2002; Zhang et al. 2004). Depending on the jet structure and the viewing angle, the same jet may be observed as different phenomena, such as short GRBs, long GRBs, X-ray flashes and X-ray rich GRBs (Yamazaki, Ioka, & Nakamura 2004, 2002; Ioka & Nakamura 2001). It is difficult to determine the jet structure from observations of the photon light curve and spectra during the GRB and afterglow phase, because the physical dimensions in these stages are much smaller than the decay lengths considered here, and the relativistic beaming prevents observing the whole angle

of the jet. TeV imaging of the β -decay emission could be a possible way⁸ to determine or constrain the jet structure, since it provides a much longer lever arm to trace the inner jet.

There are a number of uncertainties which could affect the conclusions. For instance, the photon energy density field may be higher than estimated from the diffuse backgrounds, due to contributions from the nearby H II region W49A. The latter emits about 10^{51} Lyman continuum photons s^{-1} (Conti & Blum 2002), hence the corresponding photon energy density is $\sim 10^{-14}(d_A/1 \text{ kpc})^{-2} \text{ erg cm}^{-3}$, where d_A is the distance from W49A. Since the projected distance between W49A and W49B is $\sim 40 \text{ pc}$, the IC emission within $\sim 100 \text{ pc}$ of W49B may be enhanced. Also, if the jet is directed towards us, relativistic effects such as a superluminal motion or differential Doppler boosting may be important. However, the barrel shape of W49B possibly suggests that the jet is not directed towards us. Nevertheless the forward- and counter-jet sizes may differ by factors of a few since it takes about the observed age for light to cross the system.

To infer the jet structure precisely, the sky distribution of the electrons must be nearly preserved. Thus the diffusion length of electrons has to be smaller than the emitting region. The diffusion length $r_D \sim (\kappa t_{\text{age}})^{1/2} \sim 100\gamma_{e,7}^{1/6}t_{\text{age},3.5}^{1/2} \text{ pc}$ within the remnant age t_{age} is smaller than the emitting region for $\gamma_e \sim 10^7$, if we use the diffusion coefficient of electrons $\kappa \sim 9 \times 10^{28}\gamma_{e,7}^{1/3} \text{ cm}^2 \text{ s}^{-1}$ (Wick, Dermer, & Atoyan 2004). Electrons with $\gamma_e \lesssim 10^7$ may suffer diffusion, while for $\gamma_e \gtrsim 10^9$ the emission is in the regime (b2) and the diffusion may increase the cooling region size by at most a factor 2. However we should note that the diffusion coefficient has large uncertainties.

Even if W49B is not a GRB remnant, there may exist other, older GRB remnants, whose age may be $\lesssim 10^5 \text{ yr}$, since the (collimation corrected) GRB rate is $\gtrsim 10^{-5} \text{ yr}^{-1} \text{ galaxy}^{-1}$. The same formalism may be used to discuss the detectability. As long as the electron diffusion length does not become a limiting factor, the β -decay emission from such an older remnant may be detectable.

We thank S. Razzaque, K. Mori, S. Park, J. Granot, E. Ramirez-Ruiz and the referee for useful comments. This work was supported in part by the Center for Gravitational Wave Physics under the National Science Foundation cooperative agreement PHY 01-14375 (KI, SK), NASA NAG5-13286, NSF AST 0098416 and the Monell Foundation.

⁸Other methods might include gravitational waves (Sago, Ioka, Nakamura, & Yamazaki 2004; Kobayashi & Mészáros 2003).

REFERENCES

Aharonian, F. A., & Atoyan, A. M. 2000, *A&A*, 362, 937

Aharonian, F. A., et al. 2001, *A&A*, 375, 1008

Aharonian, F. A., et al. 2002, *A&A*, 395, 803

Amenomori, M., et al. 2002, *ApJ*, 580, 887

Atoyan, A. M., & Dermer, C. D. 2001, *Phys. Rev. Lett.*, 87, 221102

Bernstein, R. A., Freedman, W. L., & Madore, B. F. 2002, *ApJ*, 571, 56

Biermann, P. L., Medina Tanco, G., Engel, R., & Pugliese, G. 2004, *ApJ*, 604, L29

Bloom, J. S., Frail, D. A., & Kulkarni, S. R. 2003, *ApJ*, 594, 674

Blumenthal, G. R., & Gould, R. J. 1970, *Rev. Mod. Phys.*, 42, 237

Conti, P. S., & Blum, R. D. 2002, *ApJ*, 564, 827

Dermer, C. D. 2002, *ApJ*, 574, 65

Dermer, C. D., & Atoyan, A. 2004, *A&A*, 418, L5

Enomoto, R., et al. 2002, *Nature*, 416, 823

Hunter, S. D., et al. 1997, *ApJ*, 481, 205

Ioka, K., & Nakamura, T. 2001, *ApJ*, 554, L163

Kaneda, H., et al. 1997, *ApJ*, 491, 638

Kinzer, R. L., Purcell, W. R., & Kurfess, J. D. 1999, *ApJ*, 515, 215

Kobayashi, S., & Mészáros, P. 2003, *ApJ*, 585, L89

Konopelko, A., Lucarelli, F., Lampeitl, H., & Hofmann, W. 2002, *astro-ph/0209431*

LeBohec, S., et al. 2000, *ApJ*, 539, 209

Lebrun, F., et al. 2004, *Nature*, 428, 293

Lessard, R. W., Buckley, J. H., Connaughton, V., Le Bohec, S. 2001, *APh*, 15, 1

McEnery, J. E., Moskalenko, I. V., & Ormes, J. F. 2004, *astro-ph/0406250*

Milgrom, M., & Usov, V. 1995, *ApJ*, 449, L37

Perna, R., & Loeb, A. 2000, *ApJ*, 533, 658

Rachen, J. P., & Mészáros, P. 1998, *Phys. Rev. D*, 58, 123005

Rossi, E., Lazzati, D., & Rees, M. J. 2002, *MNRAS*, 332, 945

Sago, N., Ioka, K., Nakamura, T., & Yamazaki, R. 2004, *Phys. Rev. D* in press, gr-qc/0405067

Snowden, S. L. 1995, *ApJ*, 454, 643

Strong, A. W., Moskalenko, I. V., & Reimer, O. 2000, *ApJ*, 537, 763

Strong, A. W., Moskalenko, I. V., & Reimer, O. 2004, *ApJ* in press, astro-ph/0406254

Vietri, M. 1995, *ApJ*, 453, 883

Vietri, M. 1998, *Phys. Rev. Lett.*, 80, 3690

Vietri, M., De Marco, D., & Guetta, D. 2003, *ApJ*, 592, 378

Waxman, E. 1995, *Phys. Rev. Lett.*, 75, 386

Waxman, E. 2004, *ApJ*, 606, 988

Waxman, E., & Bahcall, J. 1997, *Phys. Rev. Lett.*, 78, 2292

Wick, S. D., Dermer, C. D., & Atoyan, A. 2004, *Astropart. Phys.*, 21, 125

Yamazaki, R., Ioka, K., & Nakamura, T. 2002, *ApJ*, 571, L31

Yamazaki, R., Ioka, K., & Nakamura, T. 2004, *ApJ*, 607, L103

Zhang, B., & Mészáros, P. 2002, *ApJ*, 571, 876

Zhang, B., Dai, X. Y., Lloyd-Ronning, N. M., & Mészáros, P. 2004, *ApJ*, 601, L119

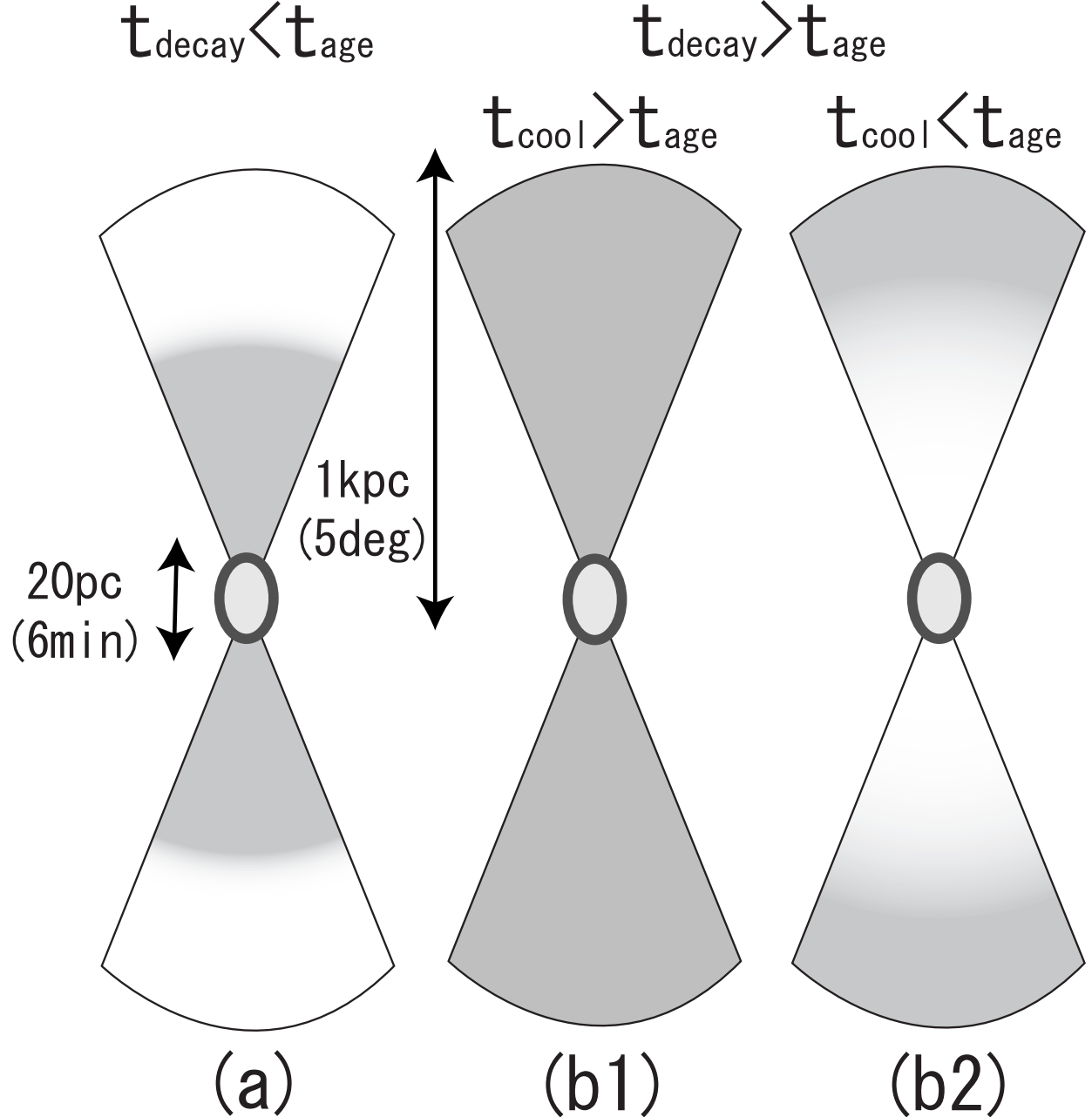


Fig. 1.— The GeV-TeV emission region (shaded region) on the sky is shown schematically. (a) The β -decay time is shorter than the remnant age $t_{\text{decay}}(\gamma_e) < t_{\text{age}}$, so that the radius of the emitting region is about the β -decay length in equation (2). The surface brightness on the sky is nearly homogeneous. (b1) $t_{\text{decay}}(\gamma_e) > t_{\text{age}}$ and the initial cooling time is longer than the remnant age $t_{\text{cool}}(\gamma_e) > t_{\text{age}}$. The radius of the emitting region is about $\sim ct_{\text{age}} \sim 1t_{\text{age},3.5}$ kpc. The surface brightness is nearly homogeneous. (b2) $t_{\text{decay}}(\gamma_e) > t_{\text{age}}$ and $t_{\text{cool}}(\gamma_e) < t_{\text{age}}$. The radius of the emitting region is about $\sim ct_{\text{age}} \sim 1t_{\text{age},3.5}$ kpc. The jet head region, of size $\sim ct_{\text{cool}}(\gamma_e)$, has a flux $\sim t_{\text{age}}/t_{\text{cool}}$ times larger than the rest. The GRB remnant W49B, shown in the center, has a radius ~ 10 pc.

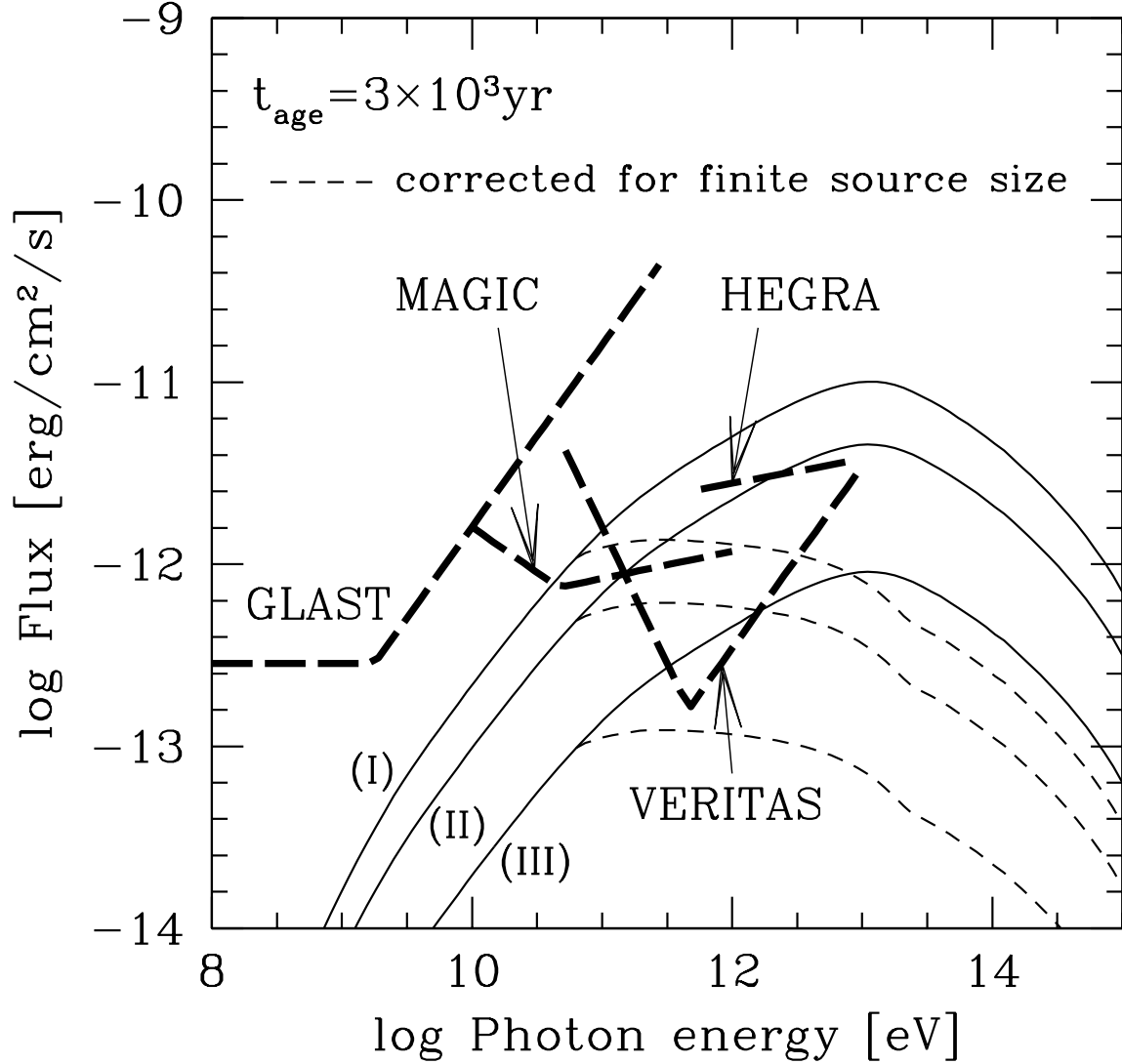


Fig. 2.— The flux of IC emission from the β -decay electrons (solid lines) is compared with the detector sensitivity (bold long dashed lines). Three cases for the total energy are plotted: (I) Neutrons in the range $10^{10} < \gamma_n < 10^{12}$ have the geometrically corrected energy 3×10^{51} erg according to equation (1). (II) The energy 3×10^{51} erg is spread among all neutrons with $1 < \gamma_n < 10^{11}$. (III) The energy of case (II) is further reduced by a factor 5. The dashed lines are the flux of β -decay emission multiplied by $(\Omega/\pi\theta_{\text{cut}})^{-1/2}$ in order to take the finite source size into account, where Ω is the solid angle of the emitting region on the sky and $\theta_{\text{cut}} \sim 0.1^\circ$ is the angular cut in the analysis. The sensitivities of HEGRA, MAGIC and VERITAS should be compared with the dashed lines. The remnant age is $t_{\text{age}} = 3 \times 10^3$ yr, and the distance is $d = 10$ kpc.